Reprint from
Springer Series in Solid-State Sciences
Volume 71: **High Magnetic Fields in Semiconductor Physics**
Editors: G. Landwehr

Springer-Verlag Berlin Heidelberg New York
London Paris Tokyo

Percolation Approach to the Quantum Hall Effect

S. Luryi

[2]AT&T Bell Laboratories, Murray Hill, NJ 07974, USA

1. Introduction

The percolation description of electron states in a 2D electron gas in strong magnetic fields was developed in refs. [1-5]. Being essentially semi-classical, this picture alone is not sufficient to give a rigorous account of the most fundamental property of the integral QHE: the extraordinary precision of quantization of the Hall conductance. Nevertheless, the percolation description appears to be quite useful in that it allows to interpret in a simple manner a number of other experimental features of the QHE and relate them to a specific model of electronic states in the presence of disorder in the sample. In this work I shall review the basic picture, following refs. [3,4] as well as some unpublished work, mostly done in collaboration with R. F. Kazarinov.

1.1 Ideal System

Consider the quantum-mechanical problem of the electronic motion in an (x,y) plane transverse to a uniform magnetic field **B**. Operators $\hat{X}$ and $\hat{Y}$ of the cyclotron-orbit-center coordinates are defined by $\hat{X} = \hat{x} + \hat{v}_y/\omega$ and $\hat{Y} = \hat{y} - \hat{v}_x/\omega$, where $\omega = eB/mc$ is the cyclotron frequency and $\hat{v}_x$, $\hat{v}_y$ are the components of the canonical velocity operator. The following commutation relations hold:

$$[\hat{v}_x,\hat{v}_y] = i\hbar\omega/m \tag{1}$$

$$[\hat{X},\hat{v}_x] = [\hat{Y},\hat{v}_y] = [\hat{X},\hat{v}_y] = [\hat{Y},\hat{v}_x] = 0 \tag{2}$$

$$[\hat{Y},\hat{X}] = i\ell^2 \tag{3}$$

where $\ell \equiv (\hbar c/eB)^{1/2}$ is the magnetic length. In virtue of (1) the spectrum of the electron kinetic energy operator $\hat{H}_0 = (m/2)[\hat{v}_x^2 + \hat{v}_y^2]$ is given by $E_n = \hbar\omega(n + \frac{1}{2})$ and because of (2) the Landau levels n are degenerate with respect to the position of the center of the cyclotron orbit. The commutation relation (3) implies that the density of states N_1 in each Landau level is given by $N_1 = (2\pi\ell^2)^{-1} = eB/hc$ states per unit area of the sample.

If there is an electric field **F** in the plane of the inversion layer, then this degeneracy is lifted. The resultant electronic states are localized in the direction of **F** by the magnetic length ℓ. In the direction of **B** the states are localized by the quantum well, while in the third direction the states are delocalized. The electronic waves propagate along the equipotential lines like light in an optical fiber. The propagation velocity turns out to be the same as the average velocity in the classical problem — the Hall velocity $v_H = c(F/B)$. It is quite easy to write down an explicit expression for these eigenstates, which I shall refer to as *fibers*. All that is important for us, however, is that they represent narrow tubes extended along equipotentials. This property remains true even in the presence of disorder, when the equipotentials are wiggly curves — contours on a topographic map — and no exact solution is available. Fortunately, we shall not need it anyway.

The QHE is an interplay between the electron density N and N_1. The *plateaus* are thought to occur when $N = N_1 \times$ *integer*, i.e., when the Fermi level E_F is positioned between two successive Landau levels, nth and $(n+1)$st. Leaving aside the question about what holds it there (the most important question!), consider what happens. First of all, there is no dissipation — large energy separates the filled and empty states. This implies $\sigma_{xx} = 0$. Electrons under the Fermi level contribute to a nondissipative Hall current. Linear density of this current J is given by $J = eN v_H = n(e^2/h)F$ and the total Hall current in the area between two electrodes biased by V is $I = n(e^2/h)V$. It is carried by electrons which are in stationary states.

1.2 Disorder Required

Disorder is of fundamental importance for the QHE. At $T=0$ the Fermi level E_F by definition coincides with the highest occupied state. In an ideal case with a uniform electron density N, the Fermi level is pinned to a Landau level at all B except for discrete values, $B_n = N\,hc/en$, at which E_F jumps between the n-th and the $(n+1)$-st level. This means that in an ideal system with no disorder, the plateaus are reduced to discrete points. The finite width of the plateaus must be attributed to pinning of the Fermi level by localized states. The nature of the localization in inversion layers in strong B is one of the most interesting consequences of studying the QHE. In what follows I shall describe a microscopic model of both localized and delocalized states, which I believe accounts for most aspects of the *integral* effect.

2. Model of Electronic States in a Disordered Sample

In our model *all electron states are fibers*, i.e., are confined within narrow tubes extended along equipotential lines. Strictly speaking, the fibers are extended along the lines of constant classical energy. The latter includes also the kinetic energy, $mv_H^2/2$, which depends on the local electric field F. Throughout this work, speaking of the equipotentials, this comment is left understood. The potential is assumed to vary smoothly on the scale of ℓ, so that at every point the sample has a well-defined Landau-level system. The existence of truly localized states with energies continuously distributed in the gaps between the local Landau levels is not required.

2.1 Global and Local Fibers

All equipotentials (and associated fiber states) distinctly fall into two classes: *global* and *local*. This distinction is especially clear in the Corbino ring geometry, where the global fibers are those which encircle the central electrode while the local can be contracted to a point by a continuous deformation. The distinction between the global and local fibers is purely *topological* and has little to do with the fiber length. A local fiber can, in fact, be quite extended — even longer than a global fiber — but it does not contribute to the Hall current.

Even though the number of current-carrying states is reduced by disorder, the current remains the same as in the ideal situation, see Fig. 1. *The entire applied voltage drops on the global states. Similarly, when the current is given, the entire Hall e.m.f. develops across the global subsystem.* Regions bounded by a local equipotential are in thermodynamic equilibrium. They may contain nonfiber states as well as local fibers revolving around potential hills and inside potential "volcanos". These regions are macroscopic and have a well-defined chemical potential E_F and a fluctuating electron

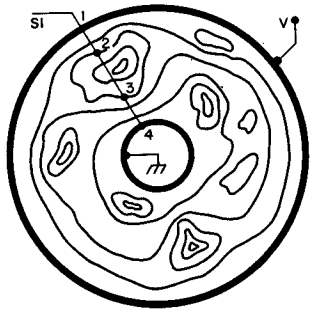

FIGURE 1: Illustration of a Corbino sample and a radial section S1, which crosses one or more isolated closed loops. Because points 2 and 3 lie on an equipotential the sum of voltages dropping in regions 1→2 and 3→4 equals the applied voltage V. The effective width of the Corbino ring in section S1 is reduced by the distance 2→3 but for a given V the Hall current does not depend on the width of the ring.

concentration. Even at $T = 0$ the Fermi level can be pinned to some of the local loops inside a macroscopic region, while the boundary of this region and an adjacent global fiber (if it exists), corresponding to a particular Landau level, can be either above or below E_F.

2.2 *Charge Fluctuations and Perfect Screening*

Let us discuss what gives rise to potential fluctuations in the inversion layer and why they can be expected to be smooth on the scale of ℓ. To be specific, we consider the GaAs/AlGaAs QHE samples. The spatial inhomogeneity of the self-consistent potential is brought about by fluctuations in the fixed positive charge responsible for the creation of the inversion layer in a heterojunction system. The fact that the Landau-level energy does indeed fluctuate, thus giving rise to patches with occupation numbers 0 or 1, is rather subtle.

Consider first an ideal situation with uniform N_+ giving rise to a partially filled Landau level and then impose a fluctuation δN_+. So long as $\delta N_+ \ll N_1$, this charge fluctuation is perfectly screened by the inversion layer, producing absolutely no spatial variation in the single-electron energy level which remains tied to E_F. This *perfect screening* is a consequence of the multiple *degeneracy* of Landau levels. A partially filled level can accommodate extra charge without changing its energy.

When $\delta N_+ > N_1$, then perfect screening does not occur and the self-consistent potential in the inversion layer fluctuates. Assume that fluctuations in the number of fixed charges N_+ per unit area are uncorrelated, $(\delta N_+/N_+) \sim (\lambda^2 N_+)^{-1/2}$, where $\lambda = \lambda(\delta N_+)$ is the spatial scale of the fluctuation. For $\delta N_+ \approx N_1$ one then has $\lambda(N_1) = \sqrt{N_+}/N_1 = \ell\sqrt{2\pi N_+/N_1}$. We see that $\lambda(N_1) \gg \ell$ provided $N_+ \gg N_1$. The crux of the matter is that the surface density N_+ of the fixed positive charge much exceeds the electron density in the inversion layer, i.e., $N_+ \gg N$ (in GaAs QHE samples N_+ is mainly compensated by a negative surface charge). Typically, N_+ results from doping a layer of thickness ~ 500 Å with donors of volume density $\sim 2\cdot 10^{18}\,\mathrm{cm}^{-3}$, i.e., $N_+ \sim 10^{13}\,\mathrm{cm}^{-2}$, while N_1 even at $B = 10$ T is only $\sim 2.4\cdot 10^{11}\,\mathrm{cm}^{-2}$. Thus the potential indeed varies smoothly on the scale of the magnetic length ℓ, which makes our model self-consistent. If N_+ were not so large, the breakdown of perfect screening would occur only at short fluctuation wavelengths and the fiber description would not be adequate.

The characteristic local fields due to the fluctuating charge by the order of magnitude are given by

$$\delta F = \frac{e\,\delta N_+}{\epsilon} = \frac{e}{\lambda\epsilon}\sqrt{N_+} \qquad (4)$$

For $\lambda \sim \lambda(N_1)$ the fluctuating field $\delta F \sim eN_1/\epsilon \gtrsim 10^4\,\mathrm{V/cm}$. Smaller fluctuating fields — those arising from large-area charge fluctutations — are typically screened by the electron gas. On the other hand, $\delta F \lesssim e\sqrt{N_+}/\epsilon d \sim 10^5\,\mathrm{V/cm}$, where d is the average distance from the inversion layer to the fluctuating fixed charges — including the thickness of an undoped AlGaAs *spacer* layer. The field due to charge fluctuations of wavelength less than d averages out without reaching the inversion layer.

2.3 *Existence of Global Fibers*

It is not at all obvious that global states do exist in a large macroscopic sample. In fact, I shall argue that in equilibrium they do not! Global states only appear in the presence of an applied Hall voltage. To see the problem, consider a random potential surface $\psi(x,y)$. Equipotentials are contour lines on the topographic map. You can probe the topology of equipotentials at any energy by filling the terrain with water and looking at the *shoreline*. At low water levels there will be *lakes in a continent*. At high levels there will be *islands in the sea*. In both limits the shoreline represents local loops. This means that neither low-energy nor high-energy equipotentials are global. There is one definite energy at which the islands-in-the-sea topology goes over into that corresponding to lakes in the continent. This energy equals $\langle\psi\rangle$ — assuming symmetric statistical properties of the random function $\psi(x,y)$ — and is called the *percolation threshold*. As we approach the transition point from the continent (sea) side the area of certain lakes (islands) diverges. It is clear that the length of the largest shoreline must also diverge at the threshold. In a finite-size sample this implies the existence of equipotentials connecting opposite edges of the sample. However, the coastline percolation in one direction (north-south) excludes the possibility of percolation in the other (east-west) direction. It is easy to see that for an uneven sample the percolation will be necessarily established in the shortest direction — radial direction in a Corbino ring.

The above argument shows that for a randomly disordered sample in equilibrium there are no global equipotentials. They begin to appear when an external voltage is applied. This is easy to visualize thinking about a *funnel* with crimped surface [4]. It has been shown [5] that at low and uniform external fields F the *fraction* of global states goes as $\sim F^p$ with $p = 41/84$. The energy range of global states may be referred to as the percolation band. Since in the presence of global equipotentials, the entire Hall voltage V develops across the global states, it follows that the percolation band emerges with a finite width equal to eV. It is the existence of global fibers that embodies the long-range order in QHE samples. Some disorder is required to establish the no-scattering situation (recall that an ideal 2DEG would give no plateaus), but too much anarchy is no good either: not every inversion layer exhibits the QHE! If one can imagine turning on the disorder at a given applied Hall voltage, then at some point one would eliminate all global fibers and the Hall current would cease. This phenomenon can be interpreted as a phase transition, in which the Hall current plays the role of an order parameter.

2.4 *Equal Occupation of Global States*

We have shown that global states constitute a small fraction of the total number of states in the inversion layer. On the other hand, the variation of the chemical potential E_F (the quasi-Fermi level) on the global states follows exactly the variation of the self-consistent potential ψ, in other words, all global states corresponding to the same Landau level are equally populated.

This can be seen as follows, Fig. 2a. Streams of the Hall current break the inversion layer into disjoint regions. Each of these regions (labelled i) is surrounded by a local

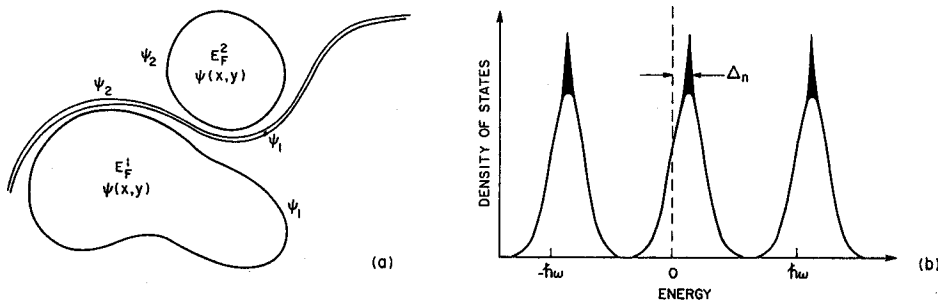

FIGURE 2: Equal occupation of global states: (a) illustration; (b) implication for the DOS

(though quite extended) equipotential ψ_i and is, therefore, in equilibrium. These regions are macroscopic, and have a well-defined chemical potential E_F^i and a fluctuating electron concentration. The average electron concentration is given by the surface density N and is the same in each macroscopic region, and hence the quantity $E_F^i - e\langle\psi\rangle_i$ has the same value throughout the sample. The gist of this argument is to note that $\psi_i = \langle\psi\rangle_i$. Indeed, the boundary of a macroscopic region is a very extended local equipotential. As such it must be close in energy to the percolation threshold $\langle\psi\rangle_i$ of region i. Since the edges of each Hall stream have the same energy ψ and chemical potential E_F as the adjacent local equipotentials, we come to the conclusion that the difference $E_F - e\psi$ is the same for all global states.

Let us plot (Fig. 2b) the density of states $D(E)$ per unit area of the sample in the presence of an applied Hall voltage V. We shall be *counting the energy of fibers from the local value of the Fermi level*, which is probably the only meaningful way to describe a system consisting of nearly independent subsystems — each of which is in a thermodynamic equilibrium by itself but not with respect to the other subsystems. If $D(E)$ is plotted in this way, it is clear that the *global* states contribute a δ-function to each $\hbar\omega$ period. The shape of $D(E)$ in the local-state region is determined by the statistical properties of the random surface $\psi(x,y)$ corresponding to the self-consistent potential. All equilibrium regions i represent statistical realizations of the same system, and hence give rise to a density of states of the same form as that in the absence of an applied voltage. In a crude approximation (neglecting correlations introduced by the screening) we can expect it to be Gaussian. With increasing V, the total area under the local-state curve changes to account for an increasing fraction of the *global* states.

2.5 *Edge States*

It has been suggested that global states may be associated with the sample edges. Indeed, the potential surface in any sample is not entirely random. In order to confine the inversion layer laterally it has to look like a trough with steep walls at the edges. There is always a global equipotential on the wall, at any energy. The associated states can give a contribution to Hall currents — revolving clockwise on one edge and counterclockwise on the other. In a particular experiment, certain fraction of the total Hall current may flow near the edges, but description of the QHE in terms of the edge currents alone, in my view, physically amounts to an untenable assumption that the quasi-Fermi level E_F is flat in the interior of the sample. In this sense, the situation is different from the description of electron diamagnetism in terms of edge currents, which is a possible, though inconvenient, description of the Landau diamagnetism [6].

In my opinion, edge states play little role in the QHE. Their number varies from one sample to another depending on the boundary conditions, but in all macroscopic

samples it remains statistically insignificant. You can think of boundary conditions for which all states near the edges are in an immediate contact with a three dimensional electron gas (e.g., a Corbino disk with source/drain implantation around the edges) — so that edge electrons can scatter into the third dimension. This will not change any experimentally observable aspect of the QHE, which is essentially a *surface* effect.

3. Consequences of the Model for the QHE

With respect to the filling of a Landau level n at a particular magnetic field and zero temperature, the sample area contains *three*, in general multiply connected, regions, Fig. 3. There are 2D patches where the n th level is filled (the n-phase), patches where this level is empty and complementary *metallic* regions — corresponding to intersecting Landau and Fermi levels.

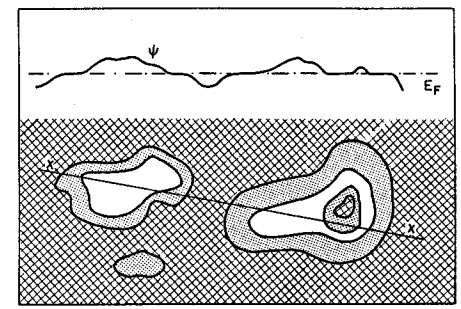

FIGURE 3: (a) Variation of the local single-electron energy $\psi(\mathbf{r})$ along a line x-x in a sample at equilibrium; (b) Three regions defined with respect to the filling of a Landau level n at zero temperature: blank area indicates the absence of n th-level electrons, cross-hatched area corresponds to completely filled regions (the n-phase), and dotted area to partially filled regions (metallic phase).

Within the n-phase the macroscopic current density J is given in terms of the gradient of the chemical potential E_F as follows:

$$J = \sigma_{xy}\, \nabla E_F \times \mathbf{B}/eB\ , \tag{5}$$

where $\sigma_{xy} = n\,e^2/h$. This can be proven as follows. Within the n-phase there are both global and local fibers. Consider a thin strip s along a global fiber. If it can be regarded as a linear conductor, its current I_s and the associated flux Φ_s of magnetic field through the contour I_s are complementary thermodynamic variables, $I_s = c\,\partial G_s/\partial\Phi_s$, where G_s is the free energy of electrons in the given strip. The single-electron contribution to the total current is given by $\delta I_s = \partial I_s/\partial N_s$, with N_s being the number of electrons in the strip. On the other hand, $\partial G_s/\partial N_s \equiv E_F^s$. Differentiating, we have $\delta I_s = c\,\partial E_F^s/\partial\Phi_s$. The minimum flux variation equals $\delta\Phi_s = hc/e$. It should be emphasized that the flux of the magnetic field through any fixed area of the ring is *not* quantized and in contrast to the situation familiar in superconductivity it can vary continuously. What is quantized in the present case is the magnetic flux through a variable area bounded by two global orbits on the chosen strip. The magnitude of the flux "quantum" follows from the periodic boundary conditions on the wave-functions of current-carrying states (which implies that the flux increment must be hc/e times an integral number $\delta\ell$) and the Principle of Least Action (whence $\delta\ell = 1$). The corresponding quantum δE_F of the chemical potential at zero temperature represents the variation of the Fermi energy across one global fiber. Therefore, $\delta I_s = (e/h)\delta E_F$ for each filled Landau level, whence we obtain (5). Note that all local fibers belong to *equilibrium* regions (surrounded by an equipotential), and hence across any local fiber $\delta E_F \equiv 0$.

Defining complex quantities $J \equiv J_x + iJ_y$ and $\tilde{F} = \nabla_x E_F + i\nabla_y E_F$, we can write (5) in the form $J = \sigma\tilde{F}$, where $\sigma \equiv \sigma_{xx} - i\sigma_{xy}$. Inasmuch as $\nabla \cdot \mathbf{J} = 0$, $\nabla \times \tilde{\mathbf{F}} = 0$, and σ is constant in the n-phase, it follows that both J and $\tilde{F}$ are analytic functions of the complex coordinate $z^* = x - iy$. Consider then a disordered sample schematically shown in Fig. 4. The total current I between the source and drain contacts equals the flux of J through any contour connecting, say, points 1 and 2. This contour can be chosen entirely within the n-phase, if the latter *percolates*, as shown in the figure. Because of the analyticity, the current is independent of the choice of a contour and equals $\sigma_{xy}\,[E_F(2) - E_F(1)]/e \equiv n(e^2/h)V$.

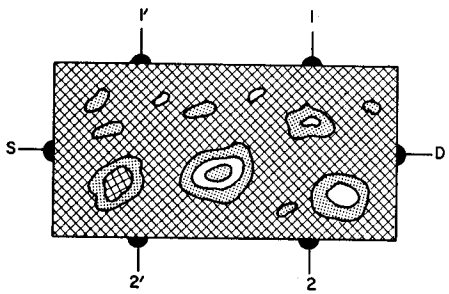

FIGURE 4: Illustration of the *on-plateau* situation. The n-phase (cross-hatched) percolates between the Hall probes. Within that phase the complex current density and chemical potential gradient are *analytic* functions of the complex coordinate.

When the magnetic field B is increased, the area of the n-phase shrinks. This occurs because $N_1 \propto B$, so that when B grows electrons fall onto the lower levels. When $N \approx (n - \frac{1}{2})N_1$, the n-phase disconnects and the metallic phase becomes percolating. The range ΔB of this inter-plateau region is proportional to the density N_G of global states in the sample, $\Delta B = (hc/e)N_G$, and therefore depends on the applied voltage (Sect. 3.2). Even at $T = 0$ the inter-plateau range can be finite. When B is increased still further, the metallic phase disconnects, the $(n-1)$-phase becomes percolating, and we have reached the next plateau.

3.1 *Plateau Width at Finite Temperatures*

Percolation model gives a simple explanation to the observed temperature dependence of the QHE plateaus. At finite T, instead of summing over *filled* global states, as we did in the preceding Section, we include the contribution of *all* global states – but weighted by their occupation probability given by the Fermi-Dirac distribution function $f = f(E_F - \psi)$ [this means we take $\delta I_s = (e/h) f\, \delta E_F$ for each global state]. In doing so, we can bring the function f out of the sum since its argument is constant on global states (Sect. 2.4). The result is an expression of the form $I = \bar{n}(e^2/h)V$, with $\bar{n}$ given by

$$\bar{n} = \sum_{n=1}^{\infty} f(\Delta_n), \tag{6}$$

where $\Delta_n = E_F(x) - \psi(x) - n\hbar\omega$ (cf. Fig. 2) is constant for each Landau level n. Transitions between the Hall plateaus are due to the variation of Δ_n with B. For an ideal situation with no disorder, global states would constitute 100% of all states and the Hall plateaus would reduce to a set of discrete points. In a real system the opposite limit occurs. The Fermi level is pinned to the global states only in a small interval ΔB.

At a nonzero T the plateaus shrink due to the washing-out of the Fermi step-function. Varying the temperature at a fixed B outside ΔB we are simply tracing the

tail of Fermi's distribution. Therefore, the temperature dependence of the deviation of R_{xy} from a quantized value at a fixed value of B must have an exponential form $\sim\exp(-E_a/kT)$, characterized by an activation energy $E_a(B) = \Delta_n$. Such behavior is indeed observed in the low-temperature experiments. The activation energy is vanishing for B inside ΔB and it grows as B is moved away from the inter-plateau range. When E_a is large, any deviation of $\bar{n}$ from an integer becomes intangible. This explains the high precision of the Hall resistance quantization.

3.2 *Voltage Dependence of the Plateau Width; Breakdown*

For typical QHE experiments the average applied field ($\sim 10^{-2}$ V/cm) is several orders of magnitude lower than the fluctuating field δF. This means that the local topography of the potential surface is only slightly modified by the applied field so that the area occupied by the local states changes very little compared to 100% at equilibrium. The *energy* range of global states was referred to as the quantum percolation band. We already know that the width of this band equals the applied Hall voltage V. Hence we can deduce qualitatively that the density N_G of global states increases with V and so does, therefore, ΔB. At the same time the plateaus *shrink*.

The exact dependence of the plateau width on V is not known — the function $N_G(V)$ may actually vary from one sample to another. Moreover, the Hall current density may be strongly nonuniform over the sample. Consider what happens if we begin to increase the voltage V applied to a Corbino ring at a fixed value of B. At a sufficiently large V the fraction of global states will approach unity $(N_G/N) \to 1$ in some section of the sample, and the Fermi level will be pinned to global fibers. This results in an *insulator-metal transition* induced by the applied field, which is observed as a breakdown of the nondissipative current flow. According to our model, it occurs when the applied field exceeds the characteristic δF of a particular sample, given by (4). Typically, $10^5 \gtrsim \delta F \gtrsim 10^4$ V/cm.

3.3 *Dissipative Current*

At $T = 0$ the n-phases can support only a non-dissipative (Hall) current, since scattering is suppressed in the completely filled Landau levels. *Metallic* regions — those corresponding to intersecting Landau and Fermi levels — are, generally, disconnected, except for discrete ranges of the magnetic field. Thus, even at a value of B for which the average N in the inversion layer corresponds to a partially filled Landau level, the potential fluctuations induce a peculiar *metal-insulator transition*. At $T = 0$ the longitudinal conductivity vanishes completely. No current can flow across filled global states due to the absence of scattering. Although, as discussed above, the area occupied by global states is small, streams of the quantum Hall current *slice* the sample into disjoint regions each of which remains at equilibrium.

At a finite temperature T in addition to the Hall current there is a longitudinal current due to generation of mobile carriers, i.e., thermal excitation of "electrons and holes" across the Landau gap $\hbar\omega$. With decreasing temperature this current goes to zero as $\exp(-\hbar\omega/kT)$. *Hopping* between local fibers across global streams also contributes to a dissipative current along the electric field. Indeed, the macroscopic equilibrium regions i are not at equilibrium *with respect to each other*. Some of the local fibers states associated with a potential hill or a potential "volcano" with its top above the Fermi level, will not be occupied. These states with energies close to the Fermi level may take part in a variable-range hopping current [7]. Temperature dependence of such conduction would be described by Mott's law $\sigma_{xx} \propto \exp[-(T_0/T)^{1/3}]$ for a two-dimensional system. At a sufficiently low temperature this path of current dominates

over the generation current. A possible indication of the hopping nature of the dissipative current is provided by experiments in which the longitudinal conductance is measured in a Corbino geometry, at a given T and a fixed applied voltage. When we measured [8] the total current between two contact islands within a high-mobility ($3\cdot10^5$cm/V·s) GaAs/AlGaAs QHE sample, separated by 1 mm and biased by 0.2 V, as a function of the magnetic field at $T=2.1$K, we found that in the range $1 \lesssim B \lesssim 4$T, the B dependence of the current at the *minima* of SdH oscillations was strictly exponential, viz. $\sigma_{xx}^{\min} \propto \exp(-B/B_0)$, with $B_0=0.328$T. (The conductivity was suppressed at still faster rate at higher B.) The exponential magnetoresistance is usually an indication of the hopping nature of the conduction [7].

4. Other Consequences

4.1 *The Density of States*

As discussed in Sect. 2.4, in the presence of a macroscopic number of global states the function $D(E)$ looks like a herd of unicorns — with one δ-function in each $\hbar\omega$ range. Now I shall argue that the animal may have another horn — at the position of the Fermi level, Fig. 5 — which moves with respect to the first when N or N_1 or even N_G are varied by external fields.

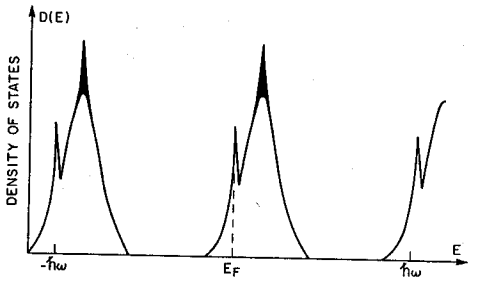

FIGURE 5: Qualitative picture of the density of states. In the presence of an applied bias V, the electronic-state energies are counted from the local value of the Fermi level. The overall shape of the peak is determined by statistical properties of the self-consistent potential at given values of B and V. The top δ-peak is proportional to the fraction of global states in the sample and hence strongly depends on V. The peak at E_F, due to the perfect screening effect, is broadened by collisions.

The appearance of a second peak in each period of the $D(E)$ is owing to the *perfect screening mechanism*, discussed in Sect. 2.2. Consider variation of the self-consistent potential $\psi(\mathbf{r})$ along some line within one of the macroscopic regions i, bounded by a local equipotential. Because region i is in equilibrium, it has a perfectly well defined E_F which is, of course, constant (dashed line in the figure). Note that a particular Landau level cannot simply cross E_F — because of the perfect screening it will be pinned to E_F until either filled or emptied. This gives a finite *measure* to the metallic regions in the sample. Their manifold still represents disconnected loops but it has acquired a finite area and contains a macroscopic fraction of electrons.

It should be realized that in this manifold *scattering is not suppressed*. Elsewhere in the sample there is no collision broadening of the Landau levels and the overall shape of $D(E)$ in our model is determined only by the inhomogeneous broadening, i.e., by the statistics of the random surface ψ. Not so in the metallic manifold — where there is a genuine lifetime broadening due to collisions. Broadening of the second peak may be describable in the self-consistent Born approximation for scattering [9] which predicts a semi-elliptic shape and a width Γ_2, which can be estimated from the relaxation time τ (related to the low-field mobility μ by $\omega\tau=\mu B/c$):

$$\Gamma_2^2 \sim \frac{2}{\pi}\hbar\omega\frac{\hbar}{\tau} = \frac{2}{\pi}(\hbar\omega)^2\frac{1}{\omega\tau} . \tag{7}$$

In the highest-mobility samples used in QHE experiments $\mu\sim10^6$ cm^2/Vsec $= 3\cdot10^8$ in gaussian units. For $B\sim10$ T $= 10^5$ gauss, $\omega\tau\sim10^3$ and hence $\Gamma_2\sim0.02\hbar\omega$.

Within the metallic manifold, the *electric* field F need not vanish — even if we neglect completely the width Γ_2. Indeed, it is the *total* single-electron energy ψ which is tied to the flat Fermi level. As mentioned at the beginning of Sect. 2, the local value of ψ includes besides the *electrostatic* potential ϕ also the kinetic energy $mv_H^2/2 \equiv (mc^2/2B^2)(\nabla\phi)^2$. Thus, in the absence of broadening ϕ must satisfy within the metallic region a nonlinear equation of the form $e\phi + (mc^2/2B^2)(\nabla\phi)^2 = \psi = E_F$. Equivalently, there is a relation for the electric field:

$$e\mathbf{F} = \frac{mc^2}{2B^2}\nabla(F^2) . \tag{8}$$

It appears that for a finite (though small) broadening, the presence of an electric field in the metallic phase is *necessary* in order to balance the diffusion flux of electrons between regions of different partial Landau-level filling.

4.2 *Fiber Inductance and Finite-Frequency Effects*

On a QHE plateau the entire externally applied voltage drops on the global fibers and drives their non-dissipative Hall current. There is a finite kinetic energy associated with the Hall current, $E = mv_H^2/2$ per electron. Because of the electron inertia it takes a finite time to charge and discharge the global fibers. The simplest way to describe these processes is to regard the fiber as an *inductive* impedance which is being charged through the Hall resistance R_{xy}.

Consider a strip of thickness ℓ along a global equipotential of length Λ. The number of filled global fibers in this strip equals $\bar{n}N_1\cdot\ell\Lambda = \bar{n}\Lambda/2\pi\ell$. The strip contributes a Hall current

$$I_s = \frac{e\,v_H}{\Lambda}\times\frac{\bar{n}\Lambda}{2\pi\ell} \tag{9}$$

The associated kinetic energy of electrons in the strip is given by

$$E_s = \frac{m}{2}v_H^2\times\frac{\bar{n}\Lambda}{2\pi\ell} \equiv \frac{1}{2}L\,I_s^2 , \tag{10}$$

whence the "fiber inductance" L is of the form

$$L = \frac{2\pi\ell\,m}{\bar{n}\,e^2}\Lambda \equiv \tau R_{xy} ; \quad \tau = \frac{m\,\ell\,\Lambda}{\hbar} . \tag{11}$$

For $\ell\sim100$Å, a delay $\tau\sim1\mu$sec corresponds to $\Lambda\sim10$ cm. Note that a global fiber because of its wiggly nature can be longer than the circumference of the sample. The reactive delay (11) can be expected to be dominant in high-frequency measurements of the conductivities from I-V characteristics.

4.3 *Magnetic Field Induced Threshold Shift in Silicon MOSFETs*

Let us first briefly discuss the MOSFET capacitance in the absence of magnetic field. The typical dependence of the differential capacitance on the gate voltage V_G is shown in the top insert to Fig. 6. Below threshold the minimum capacitance is determined by the combined thicknesses of the oxide and the semiconductor depletion region weighted by the respective permittivities. At high V_G an inversion layer appears at the

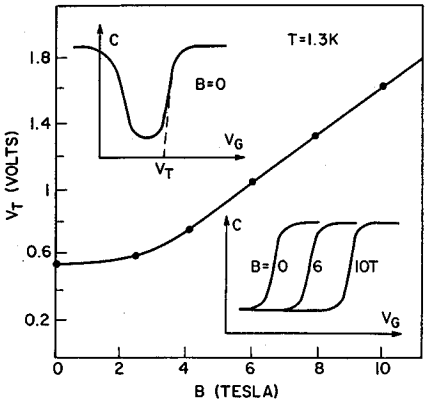

FIGURE 6: Magnetic-field induced shift of the capacitance threshold in Si MOSFET (Kazarinov and Luryi, 1982, unpublished). Experimentally [10], for $B \gtrsim 3$T the threshold is shifted linearly with B at the rate 143 mV/T. Taking the quoted value $d = 2900$Å, formula (12) gives a slope 158 mV/T.

silicon/oxide interface, which screens further penetration of the electric field into the semiconductor. In this case the differential capacitance is determined by the oxide thickness only. The gate to channel capacitance per unit area in strong inversion is given by $d(eN)/dV_G = \epsilon/4\pi d$.

The nature of capacitance threshold in strong magnetic fields is quite different. Firstly, we note that it occurs when the MOSFET is already in the strong inversion. Therefore, the threshold is associated not with a screening effect but rather with the *conductivity* of the inversion layer. In a strong magnetic field the threshold voltage V_T was found [10] to increase linearly with B, see Fig. 6. This phenomenon is another aspect of the metal-insulator transition which occurs when the *sea* corresponding to a filled Landau level breaks into disjoint *lakes*. We know that at low temperatures the partially filled Landau levels experience a percolation transition at half filling. At the lowest Landau level this transition involves the vanishing of both the longitudinal and Hall conductivities, i.e., vanishing of the total current. In this situation the inversion layer does not respond to an AC signal on the gate (of course, it does respond to DC variations in V_G). You simply cannot quickly charge the disconnected lakes by a generation or a hopping current.

The transition occurs at a critical value $N_{cr} \approx N_1/2$, The threshold voltage $V_T = V_G(N_{cr})$ is, therefore, shifted by the magnetic field as follows:

$$\frac{dV_T}{dB} = \frac{dV_G}{dN}\frac{d(N_{cr})}{dB} = \frac{e^2}{\hbar c}\frac{d}{\epsilon} = \frac{d}{137\epsilon}. \qquad (12)$$

This agrees with the experimentally measured slope [10] to better than 10%.

Acknowledgement

The percolation picture of the quantum Hall effect in the form presented here has been developed in 1981-1982 in collaboration with R. F. Kazarinov, who had originated many of the ideas described above. I am grateful to him for numerous invaluable discussions.

References

1. D.C. Tsui and S.J. Allen: Phys. Rev. B24, 4082 (1981)
1a. Y. Ono in: Anderson Localization, ed. by Y. Nagaoka and H. Fukuyama, Springer, Berlin, Heidelberg, New York (1982)
2. S. V. Iordansky: Solid State Comm. *43*, 1 (1982)
3. R. F. Kazarinov and S. Luryi: Phys. Rev. B*25*, 7626 (1982)
4. S. Luryi and R. F. Kazarinov: Phys. Rev. B*27*, 1386 (1983)
5. S. A. Trugman: Phys. Rev. B27,,7539 (1983).
6. R. Peierls: *Surprises in Theoretical Physics*, Chap. 4 (Princeton University Press, Princeton, New Jersey 1979)
7. B. I. Shklovskii and A. L. Efros: *Electronic Properties of Doped Semiconductors*, Springer Ser. Solid-State Sci., Vol. 45 (Springer, Berlin, Heidelberg 1984)
8. S. Luryi and K. K. Ng: (1982), unpublished
9. T. Ando, A. B. Fowler, and F. Stern: Rev. Mod. Phys. *54*, 437 (1982)
10. M. Kaplit and J. N. Zemel: Phys. Rev. Lett.*21*, 212 (1968)